

# The spectroscopic orbit and the geometry of R Aqr

M. Gromadzki<sup>1</sup> and J. Mikołajewska<sup>1</sup>

Nicolaus Copernicus Astronomical Center, Bartycka 18, 00-716 Warszawa, Poland  
e-mail: marg,mikolaj@camk.edu.pl

Received April ??, ???; accepted ??? ??, ???

## ABSTRACT

**Aims.** This paper is a comment on the McIntosh & Rustan (2007) and contains the proper interpretation of their result.

**Methods.** Using velocity data published by them complemented by three additional historical velocities (Merrill 1935, 1950), we have estimated the orbital parameters of symbiotic Mira R Aqr.

**Results.** We find an eccentric orbit ( $e = 0.4$ ) with a period 40.9 yr. This solution is in agreement with a resolved VLA observation of this system (Hollis et al. 1997). We also discuss the connection between orbital motion and other phenomena shown by R Aqr

**Key words.** stars: binaries: symbiotic – stars:binaries:spectroscopic – stars: individual: R Aqr

## 1. Introduction

R Aqr is a symbiotic binary surrounded by a magnificent nebula (Solf & Ulrich 1985). Both cool and hot components are unique. The cool component is a Mira variable with a pulsation period of 387<sup>d</sup> with maser emission, which is very rare, and only three among 48 symbiotics with Miras show such emission (Whitelock 2003). The hot component shows sporadic jet ejections (e.g. Kellogg et al. 2007 and Nichols et al. 2007), and Nichols et al. (2007) have also found a 1734 s periodic oscillation in Chandra X-ray observations which suggested that the hot companion is a magnetic white dwarf. Willson et al. (1981) interpreted a brightness reduction of pulsation maxima as eclipsing of the Mira by a companion surrounded by an extended gas cloud. This interpretation was supported by two facts. First, during the last hypothetical eclipse (1974-1980) a minimum was observed in the near-IR light curve similar to dust obscuration in other symbiotic Miras (e.g. Whitelock et al. 1983). Secondly, a spectrum obtained during the first such event (1886-1894) shows only faint emission lines of hydrogen and no trace of M type spectral features (Townley et al. 1928). In the historical visual light curve, there are present three phases of reduced maxima spaced by 44 yr intervals and this value was adopted as the orbital period. Additionally, the  $O - C$  diagram showed variation with a period of  $\sim 22$  yr. Wallerstein (1986) used a number of absorption spectral lines associated with the Mira in an attempt to determine the orbital elements of R Aqr. His results were consistent with the 44 yr period, but very uncertain. Hinkle et al. (1989) combined these archival data with radial velocities (RV) determined from near-IR CO and Ti I lines, and obtained a 44 yr period and a highly eccentric orbital solution.

Recently McIntosh & Rustan (2007) have collected radial velocity data of SiO maser emission of R Aqr (Lepine et al. 1978; Cohen & Ghigo 1980; Spencer et al. 1981; Lane 1982; Hall et al. 1990; Cho et al. 1996; Boboltz 1997; Hollis et al. 2000; Alcolea et al. 1999; Pardo et al. 2004; McIntosh & Rustan

2007) complemented by previous radial velocities derived from optical absorption lines (Merrill 1950; Jacobsen & Wallerstein 1975; Wallerstein 1986) and near-IR CO and Ti I lines (Hinkle et al. 1989). The astrophysical masers show series of emission lines in their spectra with various velocities associated with different maser spots around the Mira variable. Therefore, typical radial velocity of source with SiO masers is represented by velocity centroid (VC) and McIntosh & Rustan (2007) used that term in their work for all kind of velocity data. All these features are associated with the cool component or material in its close neighborhood and reflect its motion around mass center. They also estimated orbital elements using a program developed by Gudehus (2001). They obtained the correct solution but misunderstood the results, e.g. they interpreted the mass function  $f(M)$  as the total mass of the binary, which gave an unrealistic value of  $0.04 M_{\odot}$  and confused semi-major axis of the Mira orbit  $a_g \sin i$  with semi-major axis of the whole system  $a \sin i$ . Moreover, not all points listed in table 1 in this paper are plotted on their figures showing VC vs. orbital phase, namely, they lack measurement from Alcolea et al. (1999). On the figures showing VC vs. Julian days three additional points are plotted but not listed in their table. These points also did not appear on the figure with VC vs. orbital phase. In the text, authors wrote that points from Hollis et al. 2000 are listed in their Table 1, but they are not there. Neither did the authors compare the orbit solution with the resolved image of the binary (Hollis et al. 1997) nor include radial velocity measurements before 1946 (Merrill 1935, 1950). These points were also ignored in all previous papers about the orbit estimation from radial velocity (Wallerstein 1986, Hinkle et al. 1989).

This paper contains an analysis of the radial velocity data listed in Table 1 of McIntosh & Rustan (2007) together with average measurements obtained before 1946 (Merrill 1935, 1950).

## 2. Orbit determination

In order to find the orbital parameters:  $T_0$ , the time of periastron passage,  $\gamma$ , the barycentric velocity,  $K$ , the semi-amplitude,  $\omega$ ,

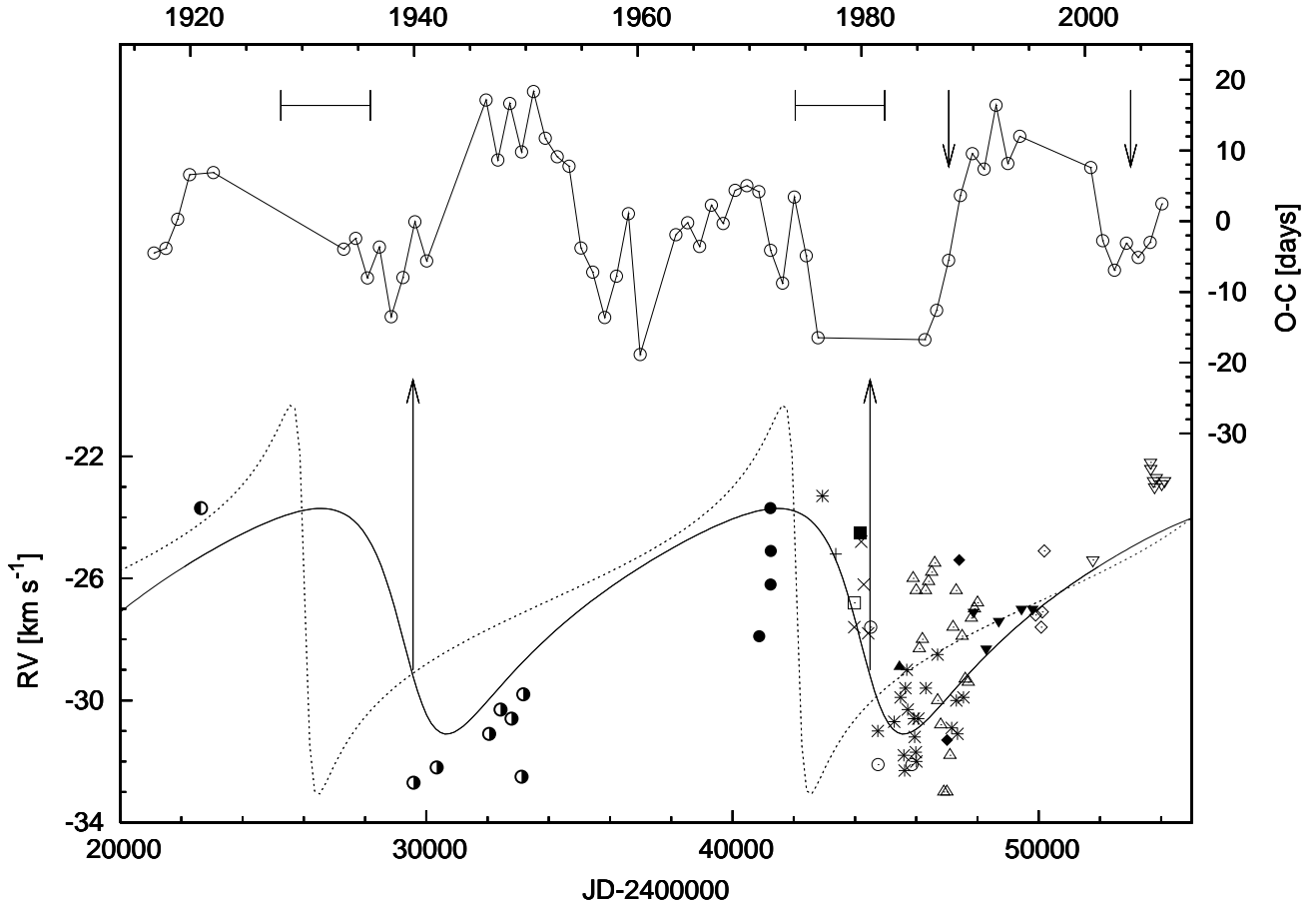


**Fig. 1.** The  $O - C$  diagram (top) and RV variations (bottom) for R Aqr. Observations from different sources are marked in the following way: Merrill 1950 (●), Merrill 1950 (○), Jacobsen & Wallerstein 1975 (●), Wallerstein 1986 (○), Hinkle et al. 1989 (\*), Lepine et al. 1978 (+), Cohen & Ghigo 1980 (■), Spencer et al. 1981 (□), Lane 1982 (×), Hall et al. 1990 (◆), Cho et al. 1996 (▲), Boboltz 1997 (◇), Alcolea et al. 1999 (△), Pardo et al. 2004 (▼), McIntosh & Rustan 2007 (▽). The solid curve represents the fitted orbital elements (solution 2 in Table 2). The dotted curve represents the orbital model proposed by Hollis et al. (1997). Bars show times of hypothetic eclipse, short arrows represent moments of jet ejection (Nichols et al. 2007), whilst long arrows show periastron passage.

the longitude of periastron, and  $e$ , the eccentricity we applied Bertiau's program (1967) based on the Lehmann-Filhés method.

The data from Table 1 of McIntosh & Rustan (2007) were supplemented by three average radial velocity measurements from Merrill (1935, 1935). These additional measurements shifted by  $-8 \text{ km s}^{-1}$  like other visual absorption lines (details in Hinkle et al. 1989) and converted to local standard of rest ( $LSR$ ) velocities are listed in Table 1. The radial velocity data are also plotted in Fig. 1. Unfortunately, these new points do not fit the 34.6 yr orbital period found by McIntosh & Rustan (2007). They fit much better the 44 yr period, although the orbital solution (with orbital period fixed at 44 yr) is still far from perfect, the orbital parameter uncertainties are really huge (e.g. 1-sigma errors for the time of periastron passage is 17 yr, and for  $\omega$ ,  $146^\circ$ , respectively). Therefore we have decided to estimate a new orbit with all parameters treated as free.

First we estimated a period of RV variations using Orfit (based on method of Schwarzenberg-Czerny 1996), and then calculated orbit with fixed period. We also decided to average SiO maser data from Cohen & Ghigo (1980), Spencer et al. (1981), Lane (1982), Alcolea et al. (1999), Hall et al. (1990), Boboltz (1997) and McIntosh & Rustan (2007) and optical observations

**Table 1.** Radial velocities of R Aqr shifted by  $-8 \text{ km s}^{-1}$  and converted to  $LSR$  before 1946

| JD      | RV [ $\text{km s}^{-1}$ ] | References   |
|---------|---------------------------|--------------|
| 2422640 | -23.7                     | Merrill 1935 |
| 2429581 | -32.7                     | Merrill 1950 |
| 2430336 | -32.2                     | Merrill 1950 |

of Jacobsen & Wallerstein (1975) in 387 day bins corresponding to the pulsation period of the Mira component. The velocity changes due to the orbital motion are negligible during such an interval. However, a single SiO measurement could be affected by other effects, e.g. asymmetries of SiO maser spot distribution around Mira. In this way, we also reduced the number of the data points from 83 to 52. The data from Hinkle et al. (1989) were not binned because they were already corrected for any velocity variation due to stellar pulsation. As a result, we obtained a highly eccentric,  $e = 0.48 \pm 0.11$ , orbit with the period of 40.5 yr and reasonable errors (solution 1 in Table 2).

We noticed that the systematic differences between average velocities from near-IR lines (Hinkle et al. 1989) and some

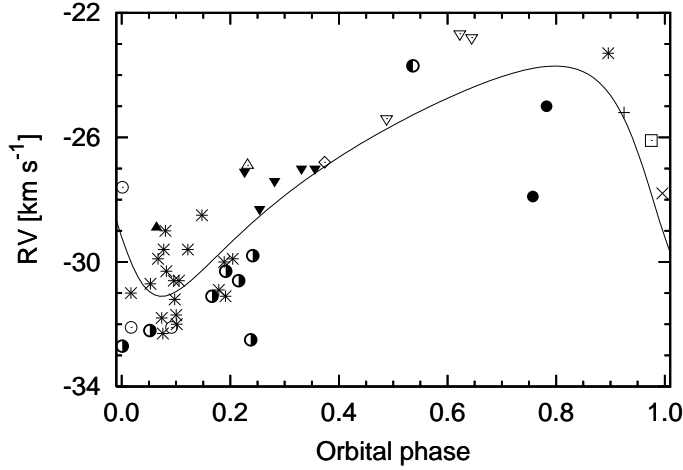


**Fig. 2.** The RV data and fitted orbital curve (solution 2 in Table 2) against orbital phase. Binned SiO maser measurements obtained in 1979 (Cohen & Ghigo 1980; Spencer et al. 1981; Lane 1982) are marked as open square ( $\square$ ). Other symbols are the same as in Fig 1. The observations from Hall et al. (1990) and Alcolea et al. (1999) have been removed. Solid curve represent our orbital solution.

velocities from SiO masers (Alcolea et al. 1999) and Hall et al. (1990) in the same bins are significant ( $4.0 \pm 1.4$ ,  $3.6 \pm 0.4$ ,  $-3.1 \pm 1.3$ ,  $-2.9 \pm 2.8$ ,  $-1.4 \pm 1$  km s $^{-1}$ ). The differences decrease with time and the last points from Alcolea et al. (1999) are similar to Pardo et al. (2004) SiO measurements. We suspect that SiO masers could be disturbed during periastron passage and then gradually rebuild (radius of SiO is 3.4 AU according to Boboltz 1997). So, we computed another orbit omitting the measurements from Alcolea et al. (1999) and Hall et al. (1990). For this set of data we got a 40.9 yr orbit with  $e = 0.40 \pm 0.09$  (solution 2 in Table 2).

The two orbital solutions (Table 2) are in fairly good agreement given their uncertainties. It is very hard to judge which one is closest to the real orbit, however for the rest of this paper we adopt the solution 2. Fig. 2 shows the data and the fitted curve (our solution 2) versus orbital phase.

Fig. 1 also compares the RV variations with the  $O - C$  for the Mira pulsations based on the visual data collected by amateur observers from AAVSO. To derive a new pulsation ephemeris, we first estimated the time of each maximum in the light curve by fitting a third order Fourier polynomial. Then a linear ephemeris:

$$\text{JD}(\text{max}) = 2\,416\,070 \pm 4 + 387.30 \pm 0.07 \times E$$

was fitted to the obtained times of maxima. The resulting  $O - C$  diagram shows a parabolic shape which corresponds to an increase in the period rate of  $0.013 \pm 0.002$  day per cycle. After subtracting this parabolic trend, a sinusoidal variation with a period of 22.5 years and amplitude of about 8 days (Fig. 2) is visible.

### 3. Discussion

Our orbital solution yields the semi-major axis of the Mira of

$$a_g \sin i = \frac{KP}{2\pi} \sqrt{1 - e^2} = 4.64^{+0.89}_{-0.84} \text{ AU},$$

and the mass function of

$$f(M) = \frac{1}{2\pi G} \cdot PK^3 (1 - e^2)^{3/2} = \frac{(M_h \sin i)^3}{(M_h + M_g)^2} = 0.0604^{+0.0347}_{-0.0248} M_\odot,$$

**Table 2.** Orbital elements for R Aqr

| Element                  | Solution 1            | Solution 2            |
|--------------------------|-----------------------|-----------------------|
| $P_{\text{orb}}$ (day)   | $14\,787 \pm 660$     | $14\,926 \pm 535$     |
| $\gamma$ (km s $^{-1}$ ) | $-26.7 \pm 0.4$       | $-26.7 \pm 0.3$       |
| $K$ (km s $^{-1}$ )      | $3.7 \pm 0.5$         | $3.7 \pm 0.4$         |
| $e$                      | $0.48 \pm 0.11$       | $0.40 \pm 0.09$       |
| $\omega$ (deg)           | $111 \pm 11$          | $119 \pm 17$          |
| $T_0$                    | $2\,444\,211 \pm 423$ | $2\,444\,491 \pm 450$ |
| $\Sigma(O - C)^2$        | 153                   | 111                   |
| $\sigma$ (km s $^{-1}$ ) | 1.80                  | 1.61                  |

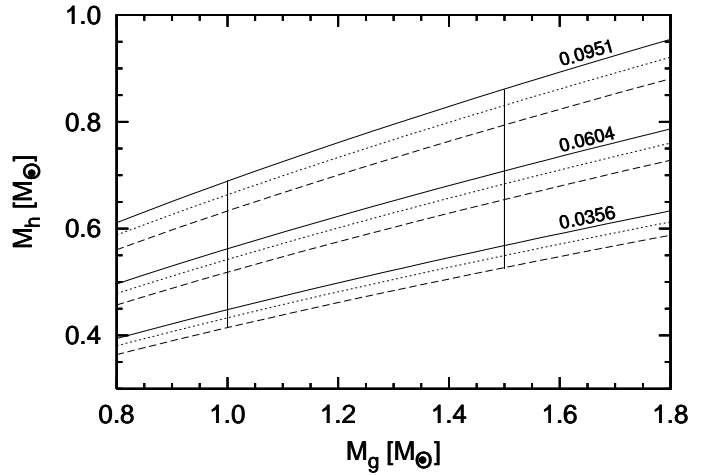


**Fig. 3.** The permitted component masses constrained by the observed mass function as well as its maximum and minimum values (solid lines labeled with the values of  $f(M)$ ), and assuming  $i = 70^\circ$ . Dotted and dashed lines show the solution for  $i = 75^\circ$ , and  $i = 90^\circ$ , respectively.

where the errors are set by uncertainties in the orbital parameters (see Table 2). The mass function sets a lower limit for the hot companion mass.

For further discussion we assume that the symbiotic binary R Aqr is composed of a Mira variable and a white dwarf (WD) companion with the orbit inclined at  $i = 70^\circ$  ( $\sim 72^\circ$  according to Solf & Ulrich 1985). Assuming plausible components masses,  $M_g = 1 - 1.5 M_\odot$ , and  $M_h = 0.5 - 1.4 M_\odot$ , for the Mira and the WD, respectively, the total mass of system  $M_{\text{tot}} = M_h + M_g$  should fall within the range  $1.5 - 3 M_\odot$ . The component masses are also limited by the orbital solution. So, if we take  $f(M) = 0.0356 - 0.0951 M_\odot$  and  $M_g = 1 - 1.5 M_\odot$  we will get  $M_{\text{tot}} = 1.5 - 2.4 M_\odot$ ,  $M_h = 0.45 - 0.86 M_\odot$  and the mass ratio  $q = M_g/M_h = 1.5 - 2.6$  (Fig. 3). These values are in good agreement with commonly adopted model of symbiotic binaries. The semi-major axis of the system,  $a$ , is of 13–16 AU which corresponds to 65–80 mas on sky for a distance,  $d = 200$  pc (see below).

Our orbital solution can be tested and refined by resolved observations of R Aqr (Hege et al. 1991; Hollis et al. 1997). In particular, the binary components of R Aqr have been resolved by VLA observations (Hollis et al. 1997) obtained on 20 Nov 1996 (JD=2 450 407). The measured separation between the VLA image in SiO maser  $v = 1$ ,  $J = 1 - 0$  transition and the continuum emission at 50 MHz associated with HII region surrounding the hot companion was  $\rho = 55 \pm 2$  mas ( $11[d/200\text{pc}]$  AU), and the position angle,  $\theta = 18^\circ \pm 2^\circ$ . This can be compared with the projected component separation on the sky plane calculated from our orbital elements.



Our preferred orbital elements (solution 2 in Table 2) combined with the orbital inclination of  $i = 70^\circ$  (Solf & Ulrich 1985) give the projected separation of  $\rho = 0.53a \sim 34\text{--}42 [d/200\text{pc}]^{-1}$  mas, and the difference between the apparent binary position angle and the position angle of the line of nodes (the binary orientation on sky),  $\theta - \Omega = -60^\circ$ . Our predicted component separation on sky is compatible with the VLA observations only if the distance is somewhat lower than 200 pc or we underestimate the  $\rho$  value due to uncertainties in our orbital elements. In fact, the predicted value of  $\rho$  will increase increasing  $e$  and/or  $\omega$ , and/or decreasing  $T_0$ . For example,  $\rho$  would increase to  $0.76a$  ( $a = 72$  mas/14.4[d/200pc] AU) by increasing  $\omega$  to 136 (by  $1-\sigma$ ), and  $\rho = 0.85a$  ( $a = 65$  mas/13[d/200pc] AU) if, in addition,  $e$  would be increased by its  $1-\sigma$  value. Similarly, using  $T_0 = 2\,444\,041$  (decreased by its  $1-\sigma$ ), and  $\omega = 136$  gives  $\rho = 0.92a$  ( $a = 60$  mas/12[d/200pc] AU). The distance to R Aqr is also relatively uncertain, and published estimates using on various methods fall into the range 180–260 pc (e.g. 180 pc by Solf & Ulrich 1985; 181 pc by Lepine et al. 1978; 240 pc using the most recent period-luminosity relation from Whitelock et al. 2008; and 260 pc by Baade 1943, 1944). The Hipparcos parallax of R Aqr is  $5.07 \pm 3.15$  mas (Perryman et al. 1997) which corresponds to a distance  $197^{+323}_{-75}$  pc. Our spectroscopic orbit is thus in a very good agreement (within  $\leq 1-\sigma$  errors in the orbital parameters) with the VLA resolved observations. The value of  $\theta = 18^\circ$ , measured with the VLA, implies  $\Omega = 78^\circ$ . Thus the position of the binary orbit on sky fits very well the general picture of the nebula around R Aqr, i.e. the orbital plane agree with plane defined by the outer “ring-like” structure (Solf & Ulrich 1985).

Our orbital solution predicts the times of spectroscopic conjunctions at  $T_{\text{conj I}} = 2\,449\,518$  (June 1994),  $T_{\text{conj II}} = 2\,444\,007$  (May 1979) for the inferior (the Mira is in front of the hot component), and the superior (the Mira behind) conjunction, respectively. The superior conjunction coincides with the last dust obscuration/eclipse (see also Fig. 4). Although the conjunction times could change by up to 1–2 years due to uncertainties of the orbital parameters, especially  $T_0$ ,  $e$  and  $\omega$ , the obscuration lasted about 6 years, and the coincidence of these two events is obvious.

Adopting plausible binary parameters, i.e. the mass ratio  $q \sim 2$ ,  $M_{\text{tot}} = 2 M_\odot$ , and  $a = 15$  AU (see above), we estimate the minimum component separation  $a(1 - e) \sim 9$  AU, and the Roche lobe radius for the Mira,  $R_L \sim 4$  AU. The near-IR interferometry of R Aqr gave the diameter of the Mira expressed as diameter of uniform disk,  $\Theta_{UD} = 14.06\text{--}20.8$  mas in  $K$ , 17.7 mas in  $J$ , and 17.7–19.07 mas in  $H$ , in intermediate and minimum pulsation phase, respectively (van Belle et al. 1996; Millan-Gabet et al. 2005; Ragland et al. 2006). These values correspond to the average radius of the Mira component,  $R_g \sim 2$  AU. So, even during periastron passage the Mira variable remains relatively far from filling Roche lobe. Many detached interacting binaries, including the symbiotic binaries as well as many X-ray binaries show evidence for much higher mass transfer rate than predicted by models of spherically symmetric wind. This phenomenon can be accounted by wind focused towards the compact component. Podsiadlowski & Mohamed (2007) proposed a model for o Cet binary system which can explain such focusing. In their model a slow wind from Mira fills Roche lobe and then the matter falls – via the  $L_1$  Lagrangian point – in accreting stream onto accretion disk around the companion. This model can be even more relevant for R Aqr where the component separation is significantly smaller than that in o Cet. In particular, it could explain the increase of extinction towards the Mira during the last 1974–1981 “eclipse” as caused by a neutral material in the accreting

stream. According to our orbital solution, the streaming material can obscure the Mira at that time, and in addition, the proximity of periastron (see Fig. 3) could give rise to enhanced mass transfer. A similar enhanced wind obscuration scenario for R Aqr was discussed by Mikołajewska & Kenyon (1992); however, in that case the source of the increased mass loss should be a helium flash above a massive core ( $M_{\text{core}} \sim 1.36 M_\odot$ ) of the Mira.

The orbital configuration of R Aqr can also explain the observations of the OH and H<sub>2</sub>O masers. The OH and H<sub>2</sub>O maser emission was detected in 1993 (Ivison et al. 1994) when the Mira was in front of the hot companion and OH and H<sub>2</sub>O masers were shielded from its radiation. Simultaneously, the maser lines were not detected in 1979 and 1984 (Cohen & Ghigo 1980; Norris et al. 1984) when the hot companion was in front of Mira.

Very intriguing is the apparent correlation between the orbital position and the  $O - C$  for the Mira pulsations. In particular, minima in the  $O - C$  diagram occur around the periastron (see Fig. 1). This may be due to some distortion of the Mira caused by tidal interaction during the periastron passage, for example if the Mira became elongated towards the hot component, the pulsation may need more time for propagation in this direction. According to our orbital model the main maximum of  $O - C$  appears close to the inferior conjunction, when the Mira eclipses the hot companion whereas the secondary, lower maximum appears in the middle of the two conjunctions when both components are well separated and we can see the elongated side.

Finally, the orbital solution proposed here is incompatible with the 17 yr orbital period for R Aqr suggested recently by Nichols et al. (2007). They noticed that radio observation obtained in 1987 and 2004 showed non-thermal spectrum which is usually a signature of a newly emitted jet (in stellar sources older jets are generally thermal), suggested that the jet formation is coupled with periastron. In our opinion such a short period seems unrealistic not only because it is not reflected by the RV variation but also because in that case there would be not enough room for a Mira with dust envelope. The 17-yr period implies a semi-major axis of  $\sim 8$  AU whereas a minimum component separation for D-type symbiotic binaries should be 10–15 AU what for typical masses (see above) indicates orbital periods longer than 20 yrs (Mikołajewska 1999). It seems that the jet ejection in R Aqr may be not connected with the orbital motion.

## 4. Conclusions

Based on published radial velocities of the Mira component we derived new orbital parameters for the symbiotic binary R Aqr. In particular, we found the orbital period of 40.9 yr, and showed that the mass function is consistent with the presence of a typical,  $1\text{--}1.5 M_\odot$ , Mira variable accompanied by a  $0.5\text{--}0.9 M_\odot$  white dwarf. We also showed that our spectroscopic orbit is compatible with the VLA astrometry (Hollis et al. 1997) and incompatible with the speckle interferometry (Hege et al. 1991). Our orbital model allow to interpret the “eclipses” of Mira as obscuration by the accretion stream. We also showed that the jet ejection (Nichols et al. 2007) is not connected with the orbital position. Finally, we note that June 2008 will be perfect for resolved imaging of R Aqr, as the Mira component will be in the minimum brightness and the separation between components on sky will be close to its maximum.

*Acknowledgements.* This study made use of the American Association of Variable Star Observers (AAVSO) International Database contributed by observers worldwide. We thank Radek Smolec for comments to the first version of this paper and Wojtek Pych for providing the Orfit software. This work

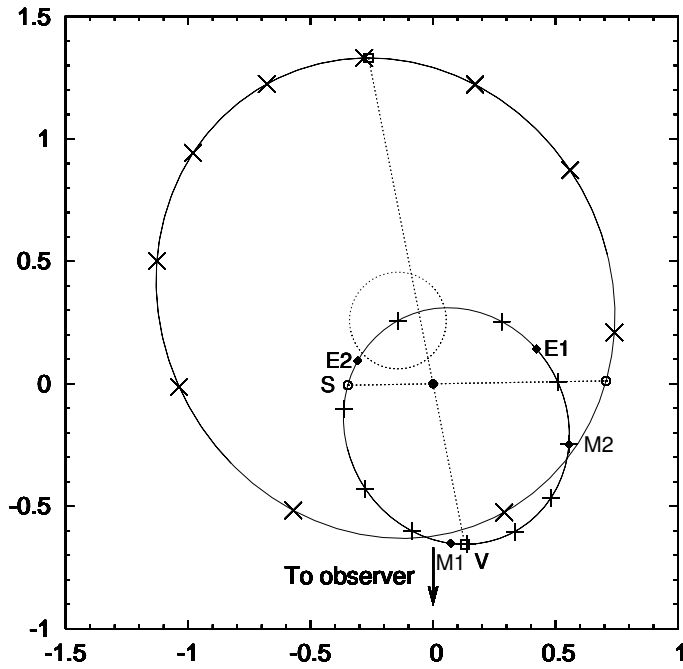


**Fig. 4.** The orbit of the Mira (+) and hot (x) component in the R Aqr binary system in steps of  $\Delta\phi = 0.1$ . In this representation, the stars move anti-clockwise. The dotted circle represents the Mira boundary at  $\phi = 0$  (periastron passage). The solid dot marks the mass center. Axes are in units of the semi-major axis  $a$ . The positions of Mira at the beginning and end of eclipse is marked by E1, and E2, respectively whereas the main and secondary maxima in  $O-C$  diagram are denoted by M1 and M2, respectively. Open squares connected with dotted line and marked by V show the component position during the VLA observation (Hollis et al. 1997). Open dots connected with dotted line and marked by S show the component position during the speckle observation (Hege et al. 1991).

was partly supported by the Polish Research grants No. 1P03D 017 27 and N203 395534.

## References

- Alcolea, J., et al. 1999, *A&AS*, 139, 461  
 Baade, W. 1943, *Carnegie Inst. Washington Yearb.*, 42, 17  
 Baade, W. 1944, *Carnegie Inst. Washington Yearb.*, 43, 12  
 Bertiau, F.C. 1967, *IAUS*, 30, 227  
 Boboltz, D. 1997, Ph.D. thesis, Virginia Polytechnic Univ.  
 Cho, S.-H., Kaifu, N., & Ukita, N. 1996, *A&AS*, 115, 117  
 Cohen, N. L., & Ghigo, F. D. 1980, *AJ*, 85, 451  
 Gudehus, D. 2001, *BAAS*, 33, 850  
 Hall, P. J., Allen, D. A., Troup, E. R., Wark, R. M., & Wright, A. E. 1990, *MNRAS*, 243, 480  
 Hege, E. K., Allen, C. K., & Cocke, W. J. 1991, *ApJ*, 381, 543  
 Hinkle, K., Wilson, T., Scharlach, W., & Fekel, F. 1989, *AJ*, 98, 1820  
 Hollis J. M., Pedelty, J. A., & Lyon, R. G. 1997, *ApJ*, 482, L85  
 Hollis, J. M., Pedelty, J. A., Forster, J., White, S., Boboltz, D., & Alcolea, J. 2000, *ApJ*, 543, L81  
 Jacobsen, T. S., & Wallerstein, G. 1975, *PASP*, 87, 269  
 Kellogg, E., Anderson, C., Korreck, K., DePasquale, J., Nichols, J., & Sokoloski, J. L. 2007, *ApJ*, 664, 1079  
 Lane, A. 1982, Ph.D. thesis, Univ. Massachusetts  
 Lepine, J., LeSqueren, A., & Scalise, E. 1978, *ApJ*, 225, 869  
 McIntosh, G. C., & Rustan, G. 2007, *ApJ*, 134, 55  
 Merrill, P. W. 1935, *ApJ*, 81, 312  
 Merrill, P. W. 1950, *ApJ*, 112, 514  
 Mikołajewska, J., & Kenyon, S. J. 1992, *MNRAS*, 256, 177  
 Mikołajewska, J. 1999, in "Optical and Infrared Spectroscopy of Circumstellar Matter", ASP Conference Series Vol. 188, eds. E. Guenther & B. Stecklum,

p.291

- Millan-Gabet, R., Pedretti, E., Monnier, J.D., Schloerb, F. P., Traub, W. A., et al. 2005, *ApJ*, 620, 961  
 Nichols, J. S., DePasquale, J., Kellogg, E., Anderson, C. S., Sokoloski, J., & Pedelty, J. 2007, *ApJ*, 660, 651  
 Norris, R. P., Haynes, R. F., Wright, A. E., & Allen, D. A. 1984, *Proc. Astron. Soc. Aust.*, 5, 562  
 Pardo, J. R., Alcolea, J., Bujarrabal, V., Colomer, F., del Romero, A., & de Vicente, P. 2004, *A&A*, 424, 145  
 Perryman, M.A.C., Lindegren, L., Kovalevsky, J., et al. 1997, *A&A*, 323, 49  
 Posiadlowski, Ph., & Mohamed, S. 2007, in "Evolution and chemistry of symbiotic star, binary post-AGB and related objects", eds. J. Mikołajewska, & R. Szczerba, *Baltic Astronomy*, 16, 26  
 Ragland, S., Traub, W. A., Berger, J.-P., Danchi, W. C., Monnier, J. D., et al. 2006, *ApJ*, 652, 650  
 Schwarzenberg-Czerny, A. 1996, *ApJ*, 460, L107  
 Solf, J., & Ulrich, H. 1985, *A&A*, 148, 274  
 Spencer, J., Winnberg, A., Olton, F., Schwartz, P., Matthews, H., & Downes, D. 1981, *AJ*, 86, 392  
 Townley, S. D., Cannon, A. J., & Campbell, L. 1928, *Ann. Harv. Coll. Obs.*, 79, 161  
 van Belle, G. T., Dyck, H. M., Benson, J. A., Lacasse, M. G. 1996, *AJ*, 112, 2147  
 Wallerstein, G. 1986, *PASP*, 98, 118  
 Willson, L. A., Garnavich, P., & Mattei, J. A. 1981, *Inf. Bull. Variable Stars*, 1961, 1  
 Whitelock, P.A. 2003, in "Symbiotic Stars Probing Stellar Evolution", ASP Conference Series Vol. 303, eds. R.L.M. Corradi, J. Mikołajewska and T.J. Mahoney, p.41  
 Whitelock, P.A., Feast, M. W., Catchpole, R. M., Carter, B. S., & Roberts, G. 1983, *MNRAS*, 203, 351  
 Whitelock, P.A., Feast, M.W., van Leeuwen, F. 2008, *MNRAS*, 386, 313/arXiv:0801.4465